Supporting Information

"Hydrogen bond locks" promoted exciton dissociation and carrier separation in co-polymers for enhancing uranyl photoreduction

Yiping Liu[a], Mei Xu[a], Mengxiong Lin[b], Maomao Zhao[a], Guihong Wu[a], Fangru Song[a], Yan Liu[a], Chengrong Zhang[a], Fengtao Yu*[ac], Jianding Qiu*[ac]

[a]*Jiangxi Province Key Laboratory of Functional Organic Polymers, East China University of Technology, Nanchang, 330013, People's Republic of China.*

[b]*China Nerin Engineering Co., Ltd, Nanchang, 330013, People's Republic of China.*

[c]*State Key Laboratory of Nuclear Resources and Environment, East China University of Technology, Nanchang, 330013, People's Republic of China.*

* Corresponding authors

* E-mail addresses: fty853815622@ecut.edu.cn (F. T. Yu); jdqiu@ecut.edu.cn (J. D. Qiu).

Table of contents

1. Experimental section

Synthesis of the monomer of 4,7-bis(4,4,5,5-tetramethyl-1,3,2-dioxaborolan-2-yl) benzo[c][1,2,5]thiadiazole (BT)

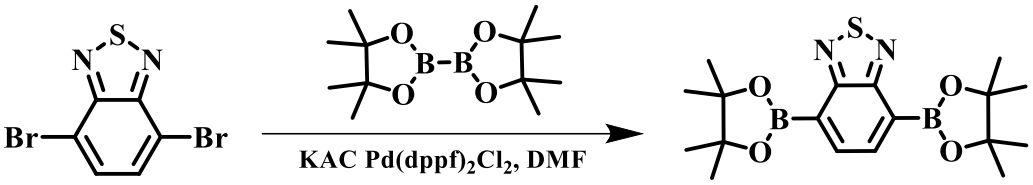

Scheme 1: Synthetic route of BT.

4,7-dibromobenzo[c][1,2,5]thiadiazole (583.6 mg, 2.0 mmol), B_2pin_2 (1270.9 mg, 5.0 mmol), KAC (1177.7 mg, 12.0 mmol), $Pd(dppf)_2Cl_2$ (220.0 mg, 2.6 mol %) and DMF (70 mL) were added into a flask (250 mL), the mixture was heated to 90 ℃ and stirred for 16 h. After cooling to room temperature (RT), the mixture was extracted by CH_2Cl_2 for three times. The combined organic layer was dried over $MgSO_4$ and evaporated to give white powder. The product was purified by column chromatography on silica gel (Petroleum ether: CH_2Cl_2 = 1:1) to give white crystal in 86 % yield. ^{1}H NMR (500 MHz, $CDCl_3$) δ 8.16 (s, 2H), 1.45 (s, 24H). ^{13}C NMR (125 MHz, $CDCl_3$) δ 156.93, 137.79, 84.42, 24.88.

Synthesis of 1,3,5-tribromo-2,4,6-trimethylbenzene (Ph-Me)

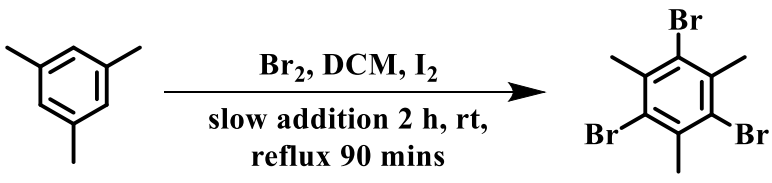

Scheme 2: Synthetic route of 1,3,5-tribromo-2,4,6-trimethylbenzene.

1,3,5-tribromo-2,4,6-trimethylbenzene was synthesized using a method adapted from a previously reported procedure. (S1) An oven-dried, 2-necked 1 L round bottom

flask (rbf) equipped with a reflux condenser and dropwise addition funnel was sealed with rubber septa. The rbf was then evacuated and back-filled with Ar (x3). To the rbf was charged: mesitylene (25.1 mL, 21.6 g, 180 mmol), anhydrous DCM (150 mL), catalytic iodine (1.37 g, 5.4 mmol), and a magnetic stir bar. A solution of bromine (36 mL, 112 g, 702 mmol) in DCM (100 mL) was added to the addition funnel and was slowly added to the stirring mesitylene solution over 2 h at room temperature. Upon addition the reaction is exothermic, yielding HBr fumes. After the addition was complete the resulting solution was refluxed (40 ˚C) for 90 mins. The mixture was then cooled to room temperature and quenched slowly with 5M NaOH (aq) (100 mL). The resulting precipitate was collected by vacuum filtration and washed with water to yield a white solid. This was then dried in a desiccator for three days. (63.8 g, 179 mmol, 99.5%) ^{1}H NMR (400 MHz in $CDCl_3$) δ: 2.66 ppm (s, 9H, Ar-CH_3). ^{13}C NMR (125 MHz, $CDCl_3$) δ 137.00, 124.99, 26.33.

Synthesis of 1,3,5-tribromo-2,4,6-trimethoxybenzene (Ph-OMe)

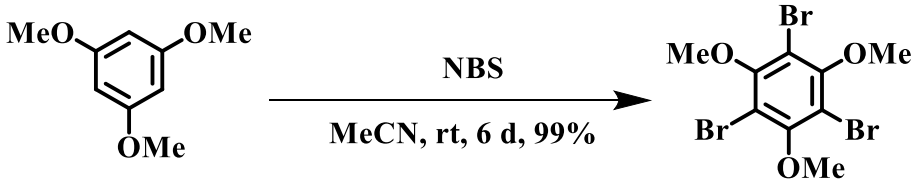

Scheme 3: Synthetic route of 1,3,5-tribromo-2,4,6-trimethoxybenzene.

A mixture of 1,3,5-trimethoxybenzene (5.00 g, 29.7 mmol) and N-bromosuccinimide (21.0 g, 118 mmol) in CH_3CN (50 mL) was stirred at room temperature for 6 d. The solvent was removed under reduced pressure, and EtOAc was added. The solution was washed with H_2O, $Na_2S_2O_4$ aq. and $NaHCO_3$ aq. The organic layer was dried over anhydrous Na_2SO_4 and filtered. The solvent was removed under

reduced pressure to give 1,3,5-tribromo-2,4,6-trimethoxybenzene (S2) quantitatively as a white powder (11.9 g, 29.3 mmol, 99%). ^{1}H NMR (400 MHz in $CDCl_3$) δ: 3.89 ppm (s, 9H, O-CH_3). ^{13}C NMR (125 MHz, $CDCl_3$) δ 154.96, 110.04, 60.67, 60.64.

Synthesis of Model-Me

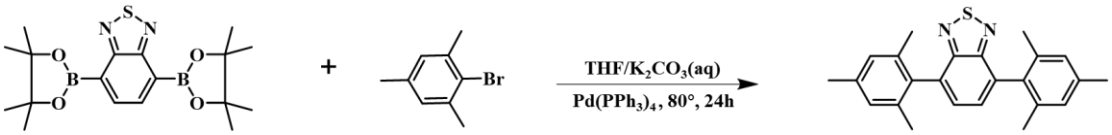

4,7-bis(4,4,5,5-tetramethyl-1,3,2-dioxaborolan-2-yl)benzo[c][1,2,5]thiadiazole (116.43 mg, 0.3 mmol), 2-bromo-1,3,5-trimethylbenzene (238.9 mg, 1.2 mmol), $Pd(PPh_3)_4$ (20 mg, 0.017 mmol), tetrahydrofuran (THF) (20 mL) and K_2CO_3 (2M 5 mL) were added into a flask (250 mL), the mixture was heated to 80 ℃ and stirred for 24 h. After cooling to room temperature (RT), the mixture was extracted by CH_2Cl_2 for three times. The combined organic layer was dried over $MgSO_4$ and evaporated to give white powder. The product was purified by column chromatography on silica gel (Petroleum ether: CH_2Cl_2 = 2:1). ^{1}H NMR (400 MHz in $CDCl_3$) ^{1}H NMR (400 MHz in $CDCl_3$) δ, ppm: 8.07 (s, 2H), 7.06 (s, 4H), 2.93 (s, 12H), 2.48 (s, 6H).

Synthesis of Model-OMe

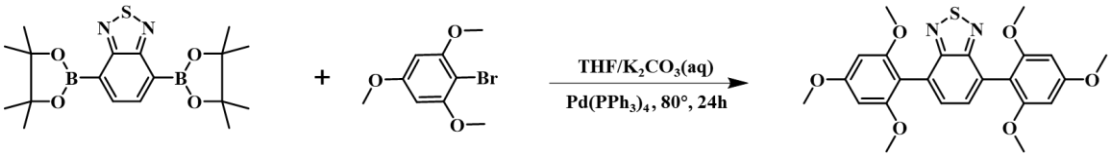

4,7-bis(4,4,5,5-tetramethyl-1,3,2-dioxaborolan-2-yl)benzo[c][1,2,5]thiadiazole (116.43 mg, 0.3 mmol), 2-bromo-1,3,5-trimethoxybenzene (296.5 mg, 1.2 mmol), $Pd(PPh_3)_4$ (20 mg, 0.017 mmol), tetrahydrofuran (THF) (20 mL) and K_2CO_3 (2 M, 5 mL) were added into a 250 mL flask, the mixture was heated to 80 ℃ and stirred for 24 h. After cooling to room temperature (RT), the mixture was extracted by CH_2Cl_2 for

three times. The combined organic layer was dried over $MgSO_4$ and evaporated to give white powder. The product was purified by column chromatography on silica gel (Petroleum ether: CH_2Cl_2 = 1:1). ^1H NMR (400 MHz in $CDCl_3$) δ, ppm: 8.58 (s, 2H), 6.24 (s, 4H), 3.90 (s, 12H), 3.84 (s, 6H).

Synthesis of CP-H, CP-Me and CP-OMe

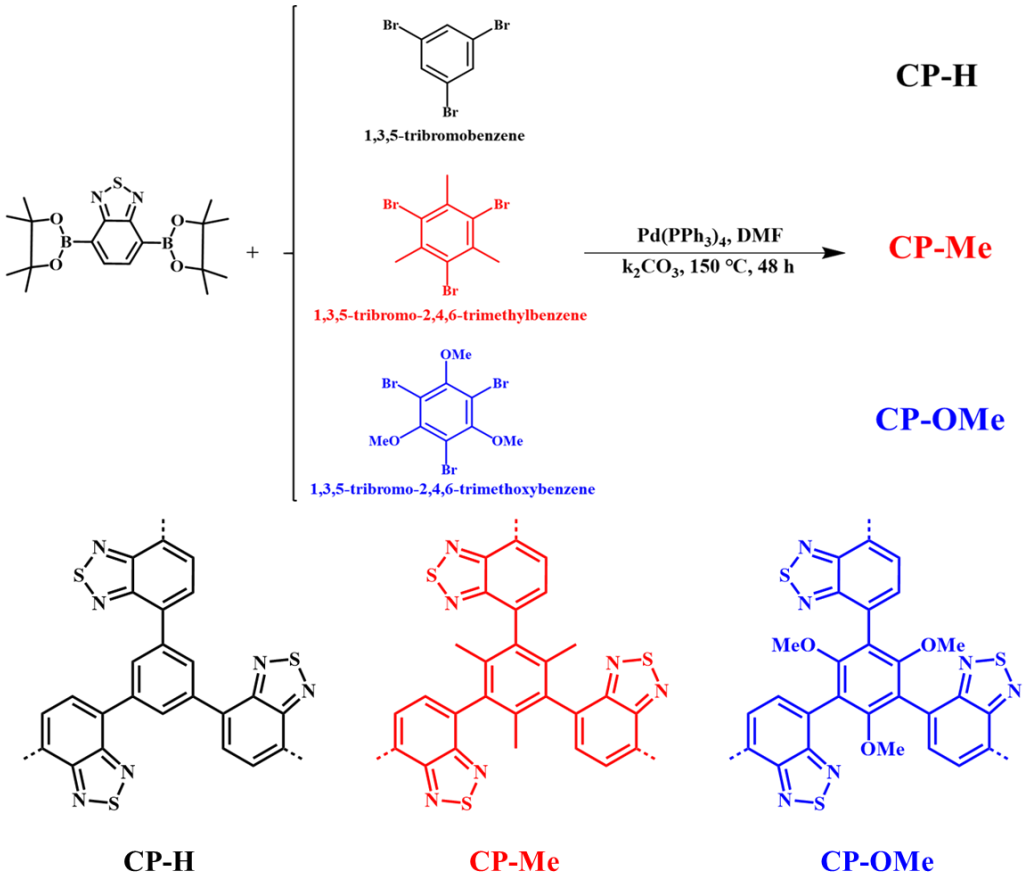

Scheme 4: Synthetic route of CP-H, CP-Me and CP-OMe.

The three target polymers (CP-H, CP-Me, CP-OMe) were synthesized by Suzuki coupling reaction. The monomers required for the synthesis are 4,7-bis(4,4,5,5-tetramethyl-1,3,2-dioxaborolan-2-yl)benzo[c][1,2,5]thiadiazole (BT), 1,3,5-tribromobenzene (Ph-H), 1,3,5-tribromo-2,4,6-trimethylbenzene (Ph-Me), 1,3,5-tribromo-2,4,6-trimethoxybenzene (Ph-OMe). The monomer BT was added to a 100 mL Shrek tube with different Ph-R respectively, then Pd catalyst, solvent DMF,

potassium carbonate was added. Solids were dissolved by sonication. The mixture was degassed using a vacuum pump and then filled with nitrogen. The reaction tube was moved to an oil bath and heated to 150 °C with stirring for 48 h. After completion of the reaction, the reaction was cooled to RT, and the crude product was post-treated by a vacuum filtration unit, and washed with deionized water, CH_3OH, DCM, and THF (100 mL of each) sequentially. To further purify the CMPs, Soxhlet extraction was carried out for 48 h with DCM, THF and methanol, respectively, until the extracts were colorless. Finally, the post-treatment product CMPs were put into a vacuum drying oven and dried at 60 °C to obtain powder. The synthetic route was shown in Scheme S4.

Synthesis of CP-H: Monomers of BT (582.15 mg, 1.5 mmol) and Py-H (311.78 mg, 1 mmol), $Pd(PPh_3)_4$ (20.0 mg) were added into solvents DMF (20 mL) and K_2CO_3 (5 mL) for polymerization. A yellowish green solid powder was obtained. The residual Pd content was found to be 0.24 wt% from ICP-MS.

Synthesis of CP-Me: Monomers of BT (582.15 mg, 1.5 mmol) and Py-Me (356.88 mg, 1 mmol), $Pd(PPh_3)_4$ (20.0 mg) were added into solvents DMF (20 mL) and K_2CO_3 (5 mL) for polymerization. A yellow-brown solid powder was obtained. The residual Pd content was found to be 0.26 wt% from ICP-MS.

Synthesis of CP-OMe: Monomers of BT (582.15 mg, 1.5 mmol) and Py-OMe (404.87 mg, 1.0 mmol), Pd $(PPh_3)_4$ (20.0 mg) were added into solvents DMF (20 mL) and K_2CO_3 (5 mL) for polymerization. A reddish-brown solid powder was obtained. The residual Pd content was found to be 0.19 wt% from ICP-MS.

2. Material

1,1'-Bis(diphenylphosphino)ferrocene]dichloropalladium(II) ($Pd(dppf)_2Cl_2$)), Potassium acetate (KAC, 98%); B_2pin_2 (99%); N, N-dimethylformamide (DMF); Mesitylene; Methylene Chloride (DCM); catalytic iodine; bromine; N-bromosuccinimide (NBS); Acetonitrile (CH_3CN); Tetrakis (triphenylphosphine) palladium ($Pd(PPh_3)_4$); potassium carbonate (K_2CO_3); 1,3,5-Tribromobenzene; arsenazo III, sodium bicarbonate ($NaHCO_3$) are obtained from Alfa Aesar Ltd. All the chemicals were commercially available, and used without further purification. Monomers of 4,7-bis(4,4,5,5-tetramethyl-1,3,2-dioxaborolan-2-yl) benzo[c][1,2,5]thiadiazole (BT), 1,3,5-tribromo-2,4,6-trimethylbenzene and 1,3,5-tribromo-2,4,6-trimethoxybenzene were prepared according to the reported methods .

3. Characterization

The synthesized monomer was checked with ^1H NMR and ^{13}C NMR spectra which were implemented in deuterated solvents on Bruker AM-400 MHz with tetramethylsilane (TMS) as an internal standard. Powder X-ray diffractions (PXRD) data were obtained on a Bruker AXS D8 Advance A25 powder X-ray diffractometer (40 kV, 40 mA) using Cu Kα (λ=1.5406 Å) radiation. FT-IR spectra were calendared with a Bruker TENSOR 27 instrument. The solid-state ^{13}C-NMR spectra were recorded on a JEOL RESONRNCE ECZ 400R NMR spectrometer at a MAS rate of 12 kHz. N_2 adsorption and desorption isotherms were carried out at 77 *K* with a micromeritics ASAP 2020 M system. The CPs samples were outgassed for 12 h at 120 °C under vacuum prior to the gas adsorption studies. The surface areas were evaluated using Brunauer-Emmett-Teller (BET) model applied between P/P_0 values of 0.05 and 0.20.

The pore size distributions were calculated using the non-localized density functional theory (NLDFT) method. UV-vis diffuse reflection spectrum (DRS) was received with UV-vis spectrophotometer (UV-2550, Shimadzu, Japan). Field-emission scanning electron microscope (FE-SEM) images were taken by Nova Nanosem 450. X-ray photoelectron spectroscopy (XPS) spectra were gathered with a Thermo VG Multilab 2000X with Al Kα irradiation. Interference ions and residual palladium concentrations were determined using an iCAP Q inductively coupled plasma mass spectrometry (ICP-MS, Thermo Fisher Scientific, USA).

4. Electrochemical measurements

A three-electrode cell was employed to measure transient photocurrent responses (*I–t*) and electrochemical impedance spectra (*EIS*) on a CHI650E (Chenhua, Shanghai) electrochemical workstation. The supporting electrolyte is 0.5 M Na_2SO_4 aqueous solution and the light source is 300 W Xe-lamp with a cutoff filter 420nm. A platinum plate and a saturated calomel electrode were employed as the counter electrode and reference electrode, respectively. The working electrodes were prepared as follows: 25.0 mg of the as-synthesized CPs were separately ground with 10 μL of a Nafion (5%) aqueous solution and 50 μL of ethanol to make slurry. The slurry was then coated onto ITO glass electrodes with an active area of 0.25 cm^2, and these electrolytes were dried at 120 °C for 1 h to evaporate the solvent in muffle furnace. The photo-current intensity of as-prepared electrodes was measured at 0 V versus Ag/AgCl with the light on and off. EIS was determined over the frequency range of 10^2–10^6 Hz with an ac amplitude of 10 mV at the open circuit voltage under room-light illumination.

5. Photocatalytic reduction of uranium experiments

Batch photocatalytic experiments were carried out in a jacketed quartz beaker photoreactor (instrument model: CEL-APR250H), and the reaction temperature is maintained at RT (20 ± 2°C) by a water-cooling system. Typically, 20.0 mg CMPs were dispersed 100 mL 50 ppm U(VI) aqueous solutions (without adding any sacrificial agents). After stirred in the dark for 60 min to reach adsorption-desorption equilibrium, then the suspension was immediately irradiated using a 300 W Xe lamp with a cut-off filter (Light source model: SHX-F300; $420 \leq \lambda \leq 780$ nm). To analysis the uranium concentration, aliquot (~2 mL) of the suspension was pipetted at given times and filtered with 0.22 μm polyether sulfone filters. The filtrate was collected and detected with UVmini-1240 by arsenazo-III spectrophotometric technology at 652 nm to determine the remaining uranium content. The removal rate is calculated according to the following formula:

$$RE = (\frac{c_0 - c_t}{c_0}) \times 100\% \quad (1)$$

where RE was uranium reduction efficiency, c_0 is initial concentration of uranium (ppm or mg L^{-1}), and c_t was the concentration of uranium (ppm or mg/L) at time, respectively.

It is worth noting that the uranium concentration in actual wastewater was determined by inductively coupled plasma mass spectrometry (ICP-MS).

In the recycling experiments: the photocatalysts were collected after the above photocatalysis experiment and subjected to ultrasound in 50 mL of 1.0 M NH_4HCO_3 with vigorous stirring for 24 h to release uranium. Then, deionized water was further used to wash the photocatalysts for the next cycle.

Selective experiments: The ions stock solutions were prepared by dissolving the corresponding nitrate salts or sodium salts of Na^+, K^+, VO_3^-, Sr^{2+}, Co^{2+}, Dy^{3+}, Yb^{3+}, Er^{3+} and Fe^{3+} in ultrapure water. U(VI) with the concentration of 50 ppm and other metal ions 4 times higher than U(VI) were used to carry out the adsorption experiment.

6. DFT calculation methods

The all geometries, including CP-H, CP-Me, CP-OMe and corresponding structures by adsorbing UO_2^{2+}, were optimized at the CAM-B3LYP/6-31G(d) level of theory using Gaussian 16. Vibrational frequency analyses were performed to confirm that the optimized structures corresponded to an energy minimum. Based on the energy with the zero-point correction, all isomers were selected for CAM-B3LYP/6-31++G (d, p) single point energy calculations. Hence, the all energy for calculating the adsorption energy were corrected by the zero-point energy. The charges were used the Mulliken population analysis at the level of CAM-B3LYP/6-31G(d). The adsorption energy (E_{ads}) was calculated as follows: $E_{ads} = -(E_{total} - E_{substrate} - E_{gas\text{-}phase\ adsorbate})$, where E_{total} is the total energy of the adsorption system, $E_{substrate}$ is the energy of the clean substrate, and $E_{gas\text{-}phase}$ adsorbate is the energy of the gas-phase molecule (UO_2^{2+}). All the above VASP calculations use the software package "Quickly use Vienna Ab-initio Simulation Package" (qvasp), which greatly improves the calculation efficiency.

7. Figures and Tables

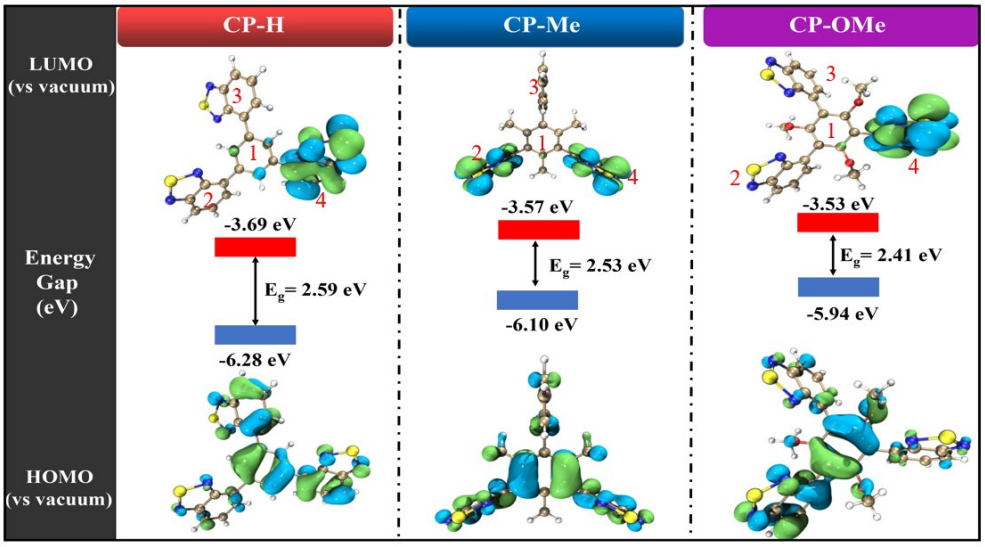

Figure S1: The HOMO and LUMO orbital distributions of polymers fragment from DFT simulation.

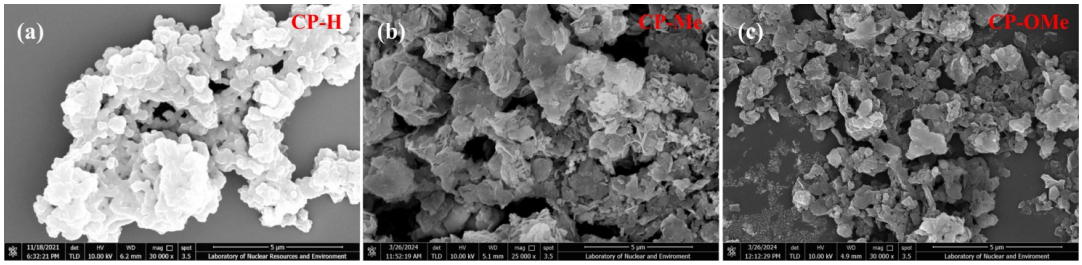

Figure S2: The SEM of CP-H, CP-Me, CP-OMe.

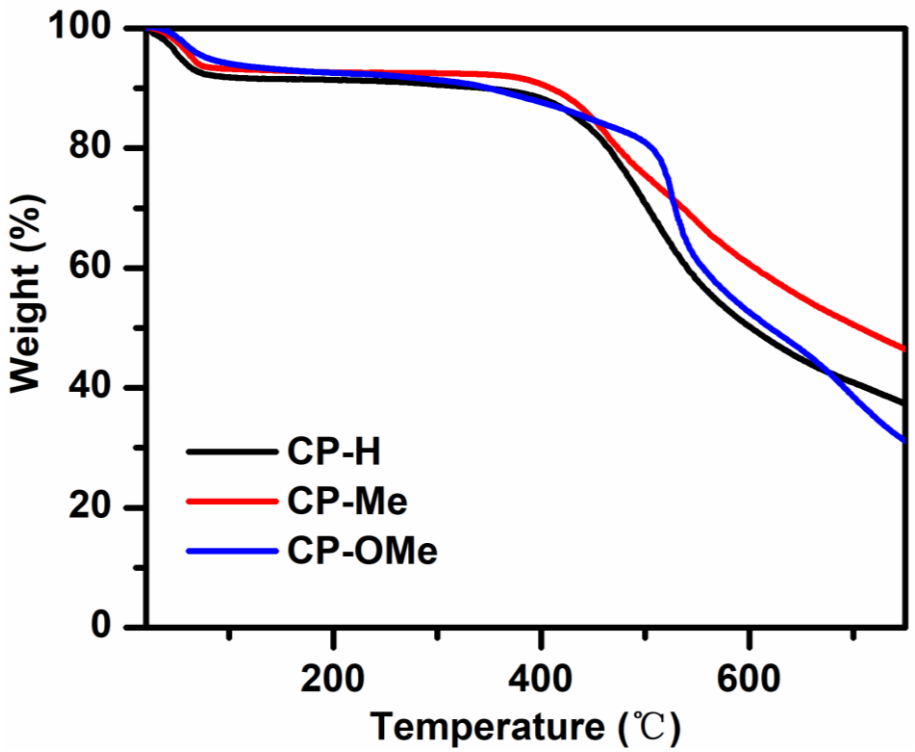

Figure S3: The thermogravimetric curve of CMPs in N_2 atmosphere.

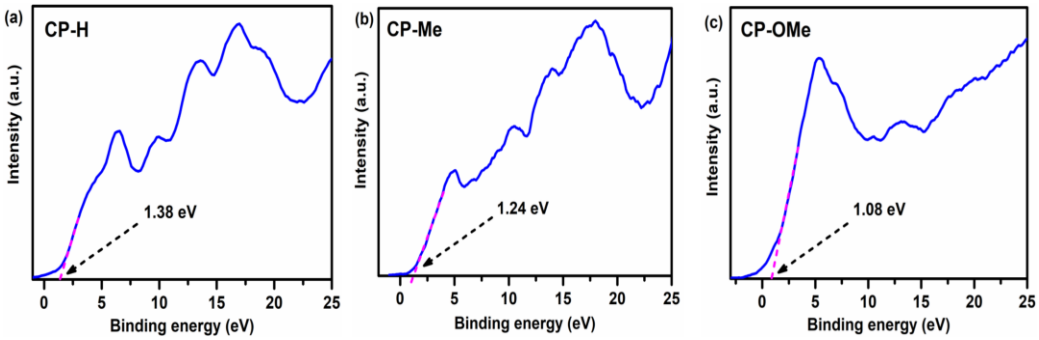

Figure S4: Valence-band XPS spectra of CP-H, CP-Me and CP-OMe.

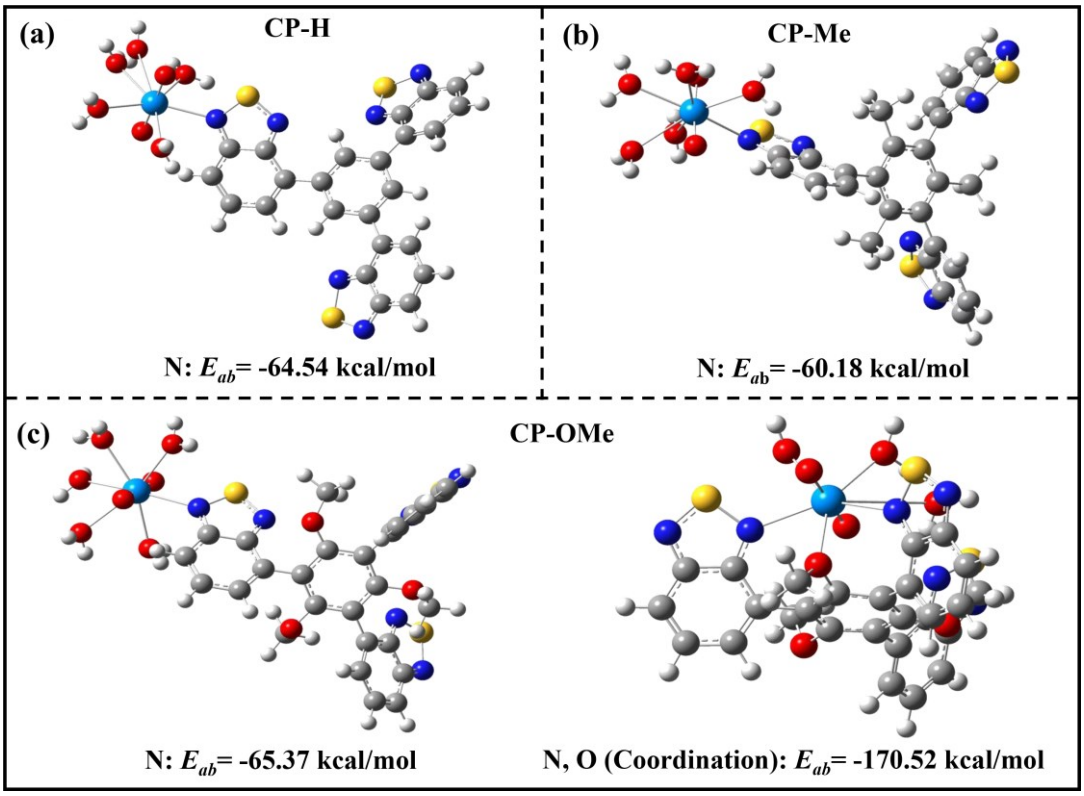

Figure S5: The optimal structure after adsorbing UO_2^{2+} and the corresponding adsorption energy.

(a) CP-H; (b) CP-Me; (c) CP-OMe.

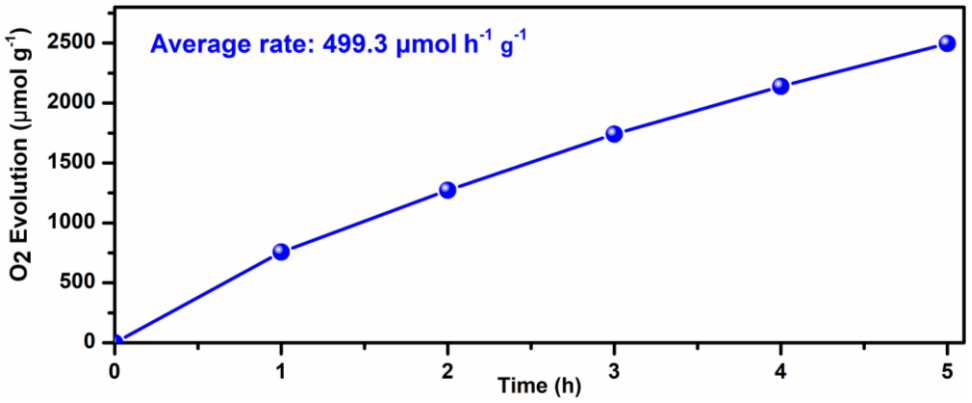

Figure S6. Time-dependent formation of O_2 in $AgNO_3$ aqueous solutions based on CP-OMe.

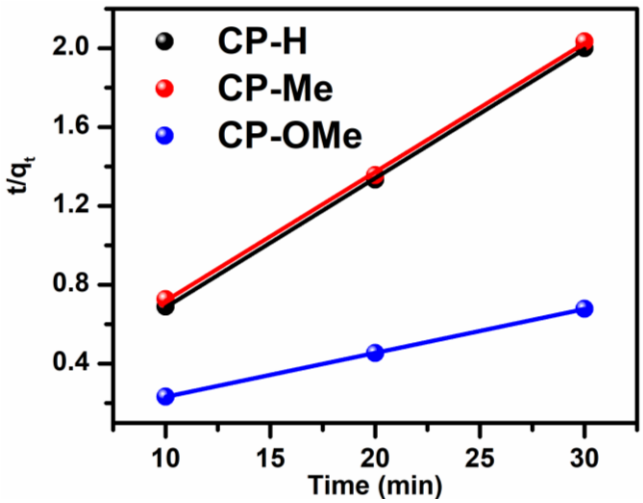

Figure S7. Pseudo-second-order kinetic plot for the adsorption under dark for CP-H, CP-Me, and CP-OMe.

Table 1. Kinetic parameters of pseudo-second-order models of uranium adsorption by means of CP-H, CP-Me and CP-OMe.

Adsorbents	**q_e, cal** ($mg \cdot g^{-1}$)	k_2 ($g \cdot mg^{-1} \cdot min^{-1}$)	k (min^{-1})	R^2
CP-H	15.27	0.054	0.001	0.999
CP-Me	15.31	0.055	0.001	0.999
CP-OMe	45.45	0.140	0.009	0.999

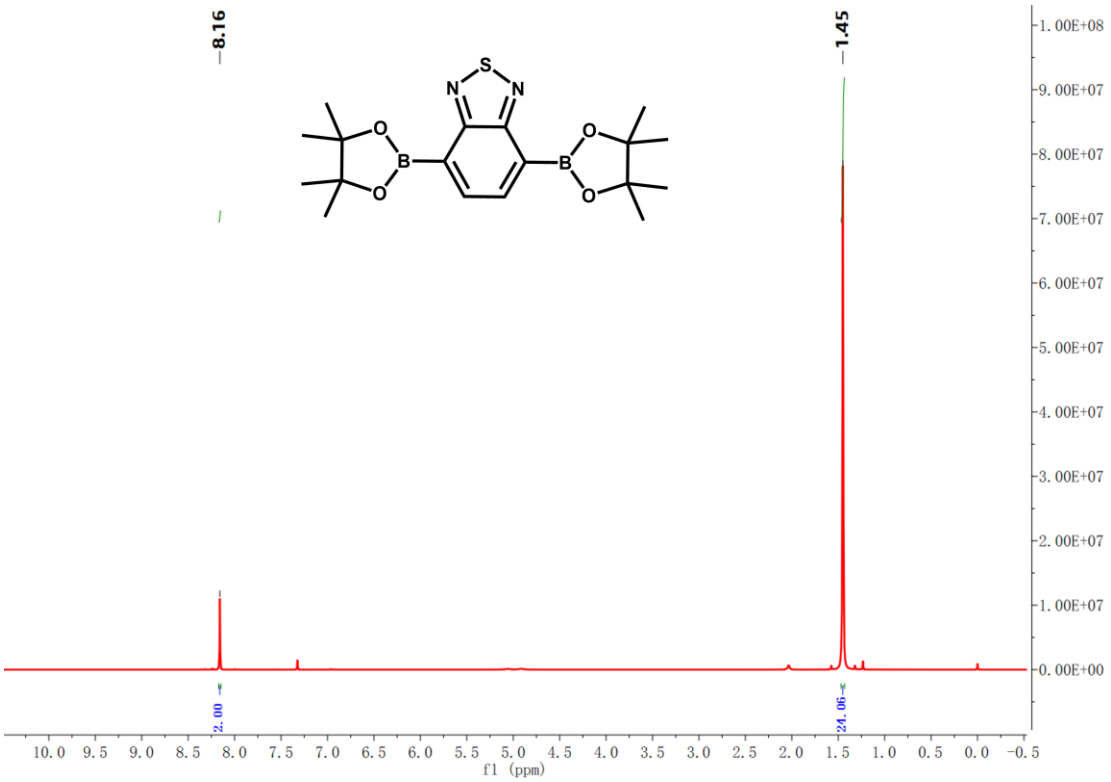

Figure S8: The ^{1}H NMR of BT in $CDCl_3$.

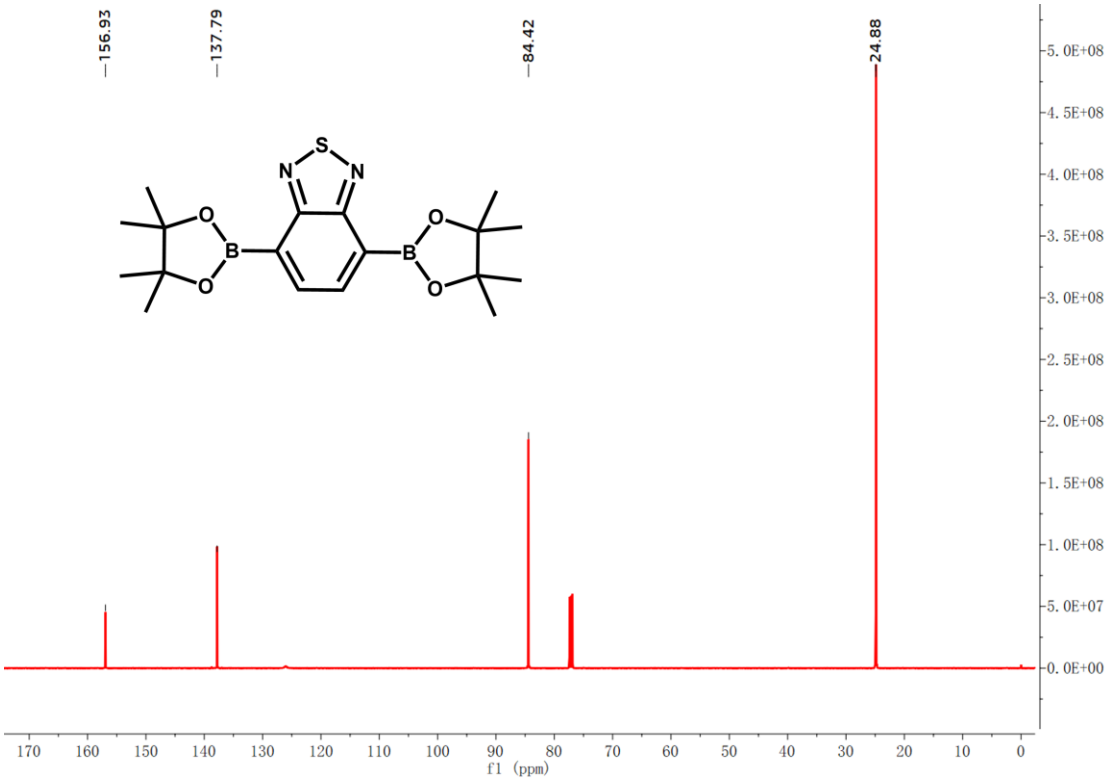

Figure S9: The ^{13}C NMR of BT in $CDCl_3$.

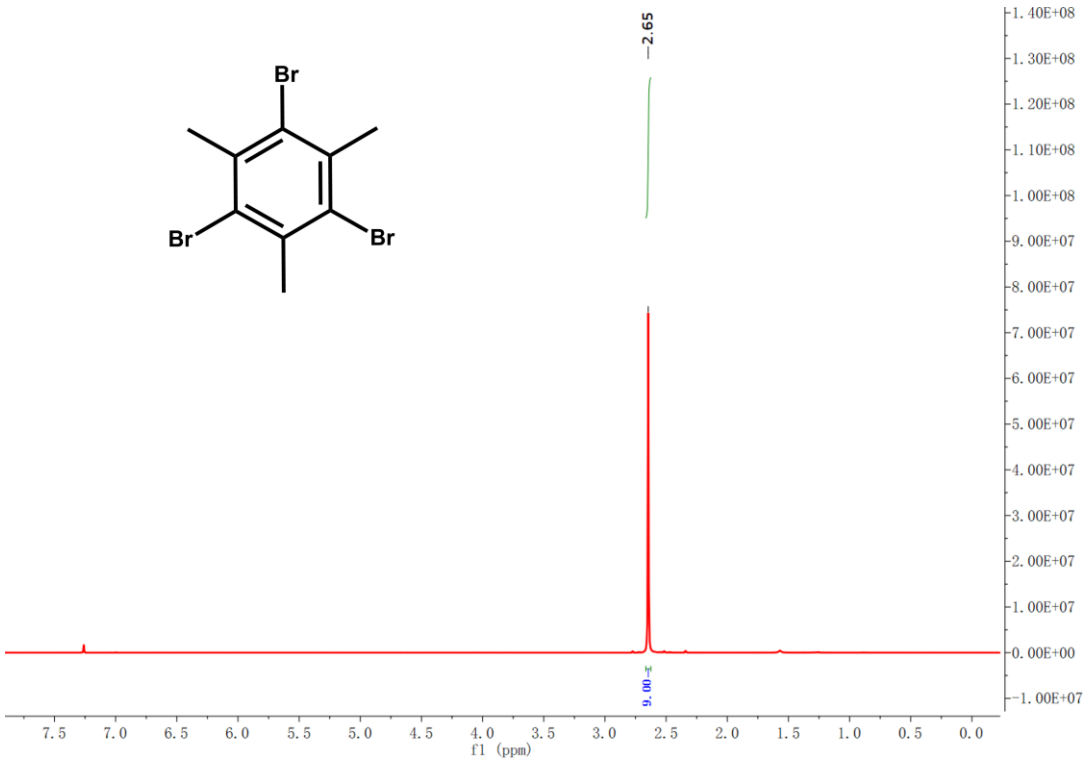

Figure S10: The ^{1}H NMR of Ph-Me in $CDCl_3$.

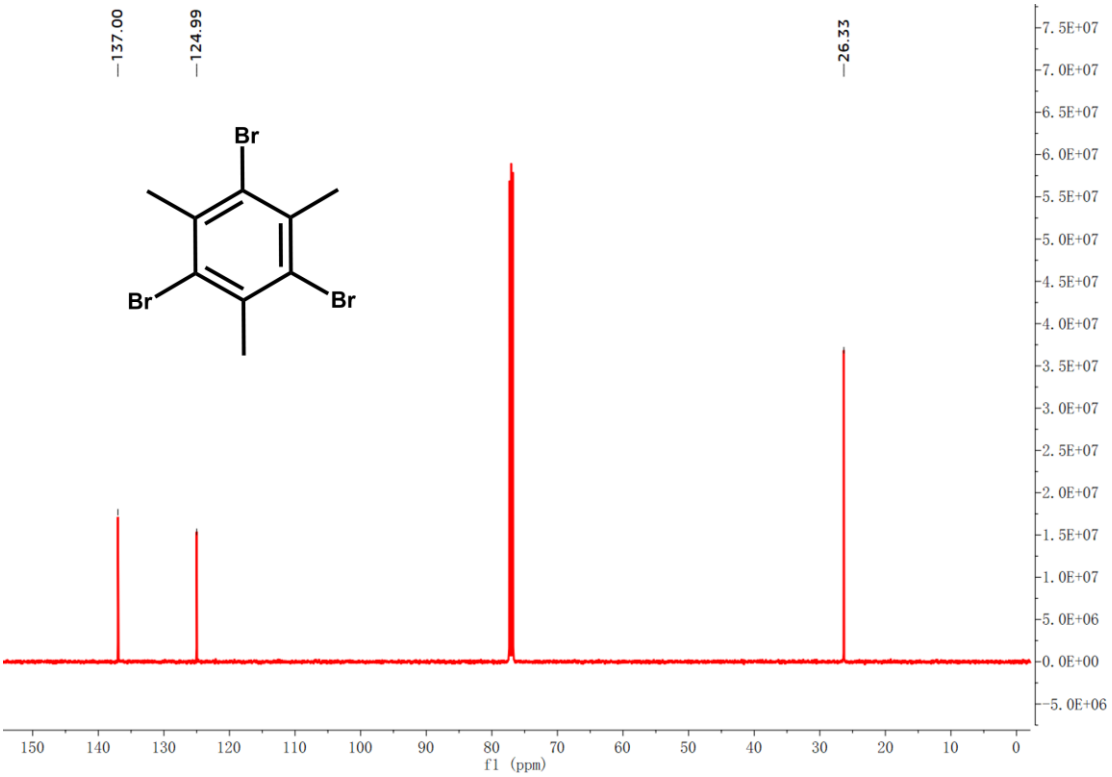

Figure S11: The ^{13}C NMR of Ph-Me in $CDCl_3$.

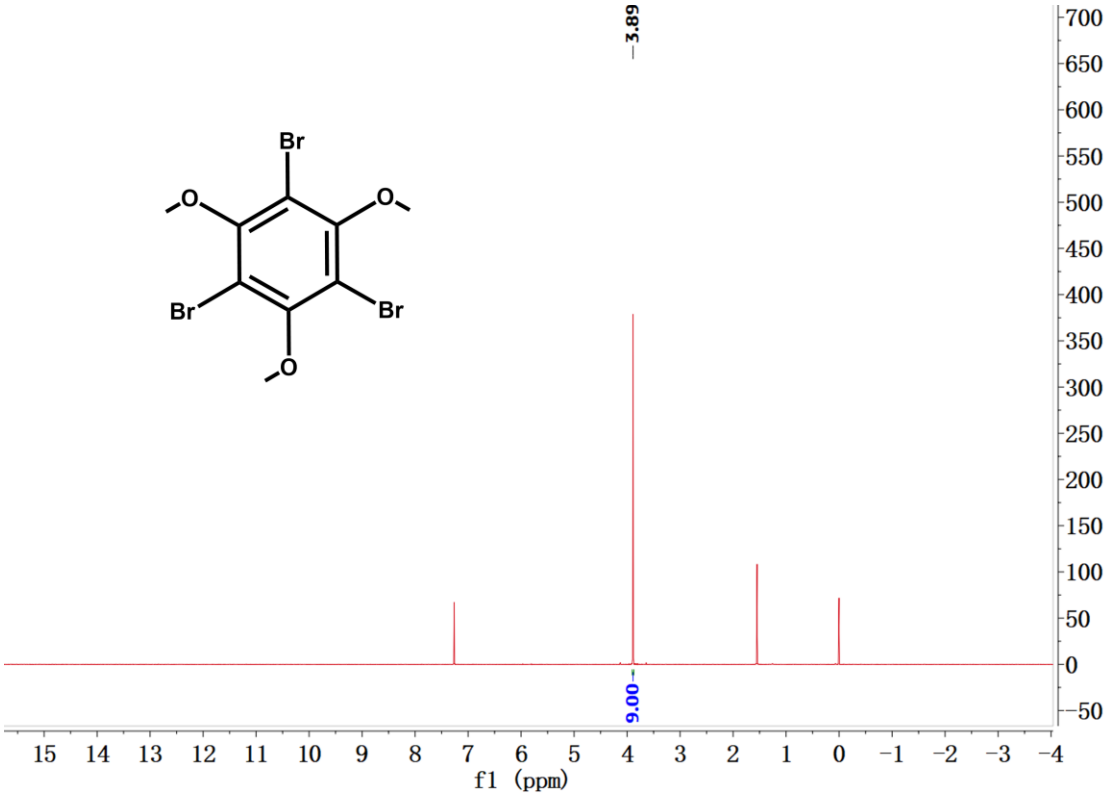

Figure S12: The ^{1}H NMR of Ph-OMe in $CDCl_3$.

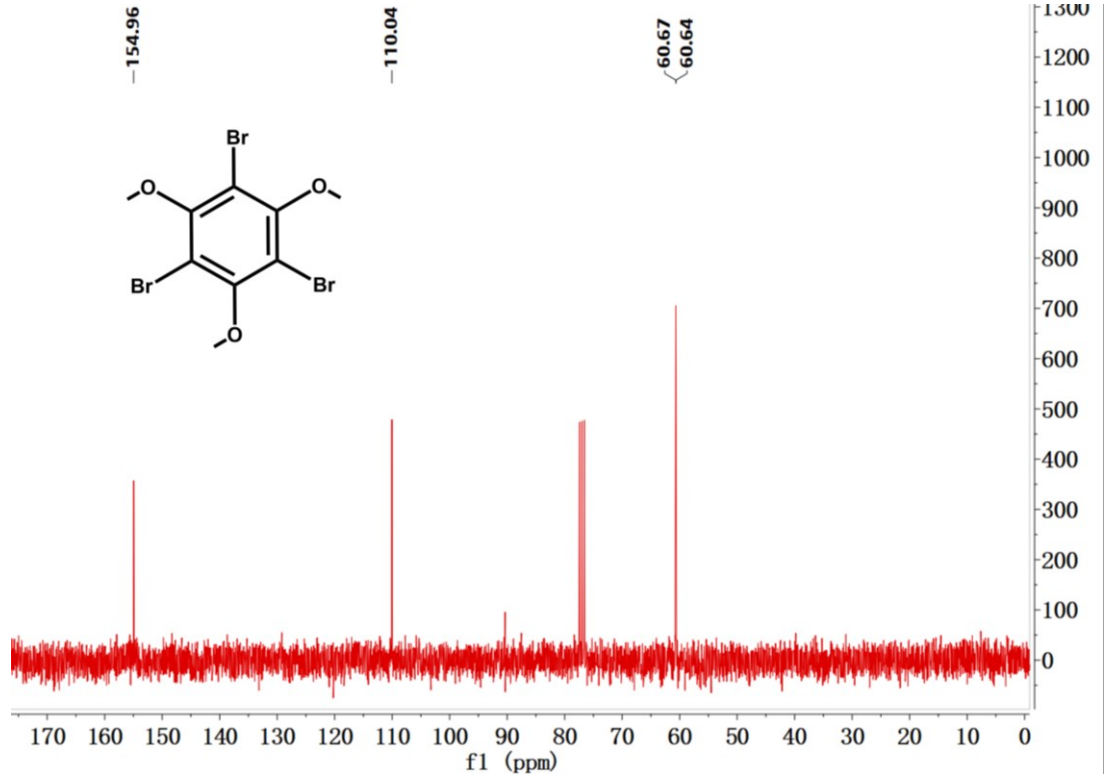

Figure S13: The ^{13}C NMR of Ph-OMe in $CDCl_3$.

Table S2: Comparison of photocatalytic activities of U(VI) on various photocatalysts.

Photocatalyst	Light source	Photocatalytic conditions	Removal rate (%)	*k*	Ref.
CP-OMe	**Vis**	**Non-sacrificial agent; 50 ppm**	**99.2 (60 min)**	**0.078**	**This work**
CP-H	Vis	Non-sacrificial agent; 50 ppm	76.4 (60 min)	0.023	This work
CP-Me	Vis	Non-sacrificial agent; 50 ppm	39.6 (60 min)	0.007	This work
Ti_3C_2/CdS	Vis	Non-sacrificial agent; 50 ppm	97 (40 min)	0.087	(S2)
CdS@NiCr-LDH-2	Vis	Non-sacrificial agent; 10 ppm	99.8 (120 min)	0.057	(S3)
MSQVZO-15	Vis	Non-sacrificial agent; 20 ppm	97 (40 min)	0.078	(S4)
ECUT-2,8-SO	Vis	Methanol; 50 ppm	63.5 (60 min)	0.014	(S5)
ECUT-4,4'-SO	Vis	Methanol; 50 ppm	85.6 (60 min)	0.029	(S5)
ECUT-3,7-SO	Vis	Methanol; 50 ppm	99.2 (60 min)	0.081	(S5)

C_3N_4	Vis	NA; 50 ppm	92 (120 min)	/	(S6)
PFB/g-C_3N_4	Vis	CH_3OH; 100 ppm,	93.7 (120 min)	0.049	(S7)
PCB/g-C_3N_4	Vis	CH_3OH; 100 ppm	99.7 (120 min)	0.037	(S7)
ECUT-C	Vis	CH_3OH; 50 ppm	72.7 (60 min)	0.022	(S8)
ECUT-CO	Vis	CH_3OH; 50 ppm	84.5 (60 min)	0.032	(S8)
ECUT-SO	Vis	CH_3OH; 50 ppm	97.8 (60 min)	0.063	(S8)
PTrSO-1	Vis	CH_3OH; 50 ppm	98.6 (120 min)	0.035	(S9)
PTrSO-2	Vis	CH_3OH; 50 ppm	99.5 (120 min)	0.044	(S9)
PTrSO-3	Vis	CH_3OH; 50 ppm	98.9 (120 min)	0.038	(S9)
PTT-Ben	Vis	AA; 50 ppm	78 (240 min)	/	(S10)
XHOF-TAQ	Sunlight	NA; 50 ppm	85 (50 min)	0.014	(S11)

Table S3: Composition and concentration of ions in uranium mine wastewater which is taken from a uranium company in China.

Composition of Sample	Concentration
U	5.8 mg L^{-1}
Th	2.1 mg L^{-1}
As	1.3 mg L^{-1}
Mn	318 mg L^{-1}
Ca	217 mg L^{-1}
Al	85 mg L^{-1}
F	304 mg L^{-1}
Ra	29 BqL^{-1}
SO_4^{2-}	1011 mg L^{-1}
COD	98 mg L^{-1}

References

(S1) Glavinović, M.; Perras, J. H.; Gelfand, B. S.; Lin, J. B.; Shimizu, G. K. H. Orthogonalization of polyaryl linkers as a route to more porous phosphonate metal-organic frameworks. *Chem. Eur. J.* **2022**, *28*, e202200874.

(S2) Liang, P. L.; Yuan, L. Y.; Du, K.; Wang, L.; Li, Z. J.; Deng, H.; Wang, X. C.; Luo, S. Z.; Shi, W. Q. Photocatalytic reduction of uranium (VI) under visible light with 2D/1D Ti_3C_2/CdS. *Chem. Eng. J.* **2021**, *420*, 129831.

(S3) Lu, S.; Yin, Y. Q.; Bao, J. C.; Wang, H. Q.; Lei, Z. W.; Hu, E. M.; Xin, Q.; Quan, Y. H.; Li, J. M.; Wang, Q. L. CdS@NiCr-LDH Z-scheme heterojunction with high adsorption-photocatalysis for

uranium (VI) removal without any sacrificial agent. *J. Environ. Chem. Eng.* **2024**, *12*, 112989.

(S4) Sun, Q. Y.; Xiao, Q. X.; Chen, Q. X.; He, W.; He, F.; Wang, H. Q. 1 T@2H-phase MoS_2 quantum dot-modified oxygen-rich vacant ZnO for the photo-reduction of uranium without sacrificial agents. *Sep. Purif. Technol.* **2024**, *345*, 127351.

(S5) Xu, M.; Liu, Y. P.; Lin, Y. T.; Zhang, J.; Liang, R. P.; Yu, S. S.; Zhang, Z. B.; Yu, F. T. Positional isomerism engineering toward minimizing exciton binding energy in sulfone copolymers for enhanced uranyl photoreduction. *Sep. Purif. Technol.* **2024**, *344*, 127259.

(S6) Wang, H. H.; Guo, H.; Zhang, N.; Chen, Z. S.; Hu, B. W.; Wang, X. K. Enhanced Photoreduction of U(VI) on C_3N_4 by Cr (VI) and Bisphenol A: ESR, XPS, and EXAFS Investigation. *Environ. Sci. Technol.* **2019**, *53*, 6454–6461().

(S7) Yu, F. T.; Yu, Z. W.; Xu, Z. Z.; Xiong, J. B.; Fan, Q. W.; Feng, X. F.; Tao, Y.; Hua, J. L.; Luo, F. Heteroatom engineering of polymeric carbon nitride heterojunctions for boosting photocatalytic reduction of hexavalent uranium. *Mol. Syst. Des. Eng.* **2020**, *5*, 882-889.

(S8) Yu, F. T.; Zhu, Z. Q.; Wang, S. P.; Peng, Y. K.; Xu, Z. Z.; Tao, Y.; Xiong, J. B.; Fan, Q. W.; Luo, F. Tunable perylene-based donor-acceptor conjugated microporous polymer to significantly enhance photocatalytic uranium extraction from seawater. *Chem. Eng. J.* **2021**, *412*, 127558.

(S9) Yu, F. T.; Zhu, Z. Q.; Wang, S. P.; Wang, J. Y.; Xu, Z. Z.; Song, F. R.; Dong, Z. M.; Zhang, Z. B. Novel donor-acceptor-acceptor ternary conjugated microporous polymers with boosting forward charge separation and suppressing backward charge recombination for photocatalytic reduction of uranium (VI). *Appl. Catal. B Environ.* **2022**, *301*, 120819.

(S10) Chen, B.; Zhang, G. K.; Chen, L.; Kang, J. Y.; Wang, Y. H.; Chen, S. Y.; Jin, Y. D.; Yan, H. J.; Xia, C. Q. Visible light driven photocatalytic removal of uranium (VI) in strongly acidic solution.

J. Hazard. Mater. **426**, 127851 (2022).

(S11) Feng, L. J.; Yuan, Y. H.; Yan, B. J.; Feng, T. T.; Jian, Y. P.; Zhang, J. C.; Sun, W. Y.; Luo, G. S.; Wang, N. Halogen hydrogen-bonded organic framework (XHOF) constructed by singlet open-shell diradical for efficient photoreduction of U(VI). *Nat. Commun.* **2022**, *13*, 1389.